Defect and Diffusion Forum
ISSN: 1662-9507, Vol. 373, pp 65-70
doi:10.4028/www.scientific.net/DDF.373.65

Submitted: 2015-10-13
Revised: 2016-07-19
Accepted: 2016-07-27
Online: 2017-03-24

Spin-Polarized Positron Annihilation Study on Some Ferromagnets

H. Li, M. Maekawa, A. Miyashita, A. Kawasuso[a *]

National Institutes for Quantum and Radiological Science and Technology,
1233, Watanuki, Takasaki, Gunma 370-1292, Japan

[a]kawasuso.atsuo@qst.go.jp

Keywords: Spin, Ferromagnets, Momentum distribution, Band structure

Abstract. We briefly review the spin-polarized positron annihilation experiments on some ferromagnets (Fe, Co, Ni, Gd, Co_2MnSi, Co_2MnAl and NiMnSb) using positron beams generated with ^{68}Ge-^{68}Ga sources. The differential DBAR spectra between majority and minority spin electrons are well interpreted by the first principles band structure calculation. This further provides information about the half-metallicity of the Heusler alloys. The surfaces of Fe, Co and Ni are more negatively spin-polarized, that is, there are more majority than minority spin electrons. To explain the observed spin polarization quantitatively, detailed theoretical calculations and further experiments are required.

Introduction

After the discovery of parity non-conservation in the weak interaction, spin-polarized positron annihilation spectroscopy (SP-PAS) based on angular correlation of annihilation radiation method has been used for the study of ferromagnetic band structure [1]. We recently demonstrated that the Doppler broadening of annihilation radiation (DBAR) can also be used for the same purpose [2, 3]. To examine the differential DBAR spectrum between majority and minority spin bands, like the magnetic Compton profiling, the spectra obtained in positive and negative magnetic fields should be renormalized to the spin-dependent annihilation rates. Although this issue had ever been pursued using three-gamma annihilation intensity [4], the further studies are still needed.

In 1980, the spin polarization of Ni surface was determined through spin-polarized positronium annihilation experiment [5]. However, afterwards, no further researches have been made. Considering the recent progress in spintronics field, we revive this technique with its applications to giant spin-Hall systems, Rashba systems and topological insulators. But, there are still open questions about application of this technique [6-8]. For instance, the reasons for the significantly small surface spin polarization of Ni (only a few %) [5] have not yet been revealed.

In the first section of this paper, we examine the differential DBAR spectra between majority and minority spin electrons from classical ferromagnets to some Heusler alloys with the first principles band structure calculation. In the second section, we summarize the results on the surface spin polarizations of Fe, Co and Ni determined by the positronium annihilation method.

Doppler broadening of annihilation radiation

In this section, we present the results on spin-polarized DBAR study on ferromagnets. The principle is as follows. The differential DBAR spectrum between majority and minority spin bands is given by

$$N_{maj}(p_z) - N_{\min}(p_z) = [N_+(p_z) - N_-(p_z)] + P_+ \frac{\lambda^{\Uparrow} - \lambda^{\Downarrow}}{\lambda^{\Downarrow} + \lambda^{\Uparrow}} [N_+(p_z) + N_-(p_z)], \quad (1)$$

where $N_+(p_z)$ and $N_-(p_z)$ are the DBAR spectra in positive and negative magnetic fields, respectively, P_+ denotes the polarization of positrons and $\lambda^{\Uparrow(\Downarrow)}$ is the total annihilation rate of spin-up (spin-down) positrons:

$$\lambda^{\Uparrow(\Downarrow)} = \lambda_{man(\min)} + (\lambda_{man(\min)} + 2\lambda_{\min(maj)})/1115, \quad (2)$$

where $\lambda_{maj(min)}$ is the two-gamma annihilation rate of positrons with majority and minority spin electrons. These are determined from two-gamma annihilation rate in positive (negative) magnetic field ($=1/\tau_{\pm}$) given by

$$\lambda_{\pm} = (1 \pm P_{+})\lambda_{maj}/2 + (1 \mp P_{+})\lambda_{\min}/2 . \quad (3)$$

We measured polycrystalline Fe, Co, Ni, Gd, Co_2MnSi (CMS), Co_2MnAl (CMA) and NiMnSb (NMS) samples with thicknesses of 1~2 mm and purities of 99.9~99.999%. These samples were electrochemically polished and subjected to heat treatment at 1200 ^{o}C (Fe, Co, Ni), 1100 ^{o}C (Gd) and at 800 ^{o}C (CMS, CMA and NMS). The x-ray diffraction 2θ measurement showed that the CMS sample was in a mixture of ordered $L2_1$ and M-S disordered B2 structures, the CMA sample was completely in M-A disordered B2 structure and the NMS sample was in ordered $C1_b$ structure. Using a Ge detector and a ^{68}Ge-^{68}Ga source, DBAR spectra were measured at room temperature in magnetic field of ±1 T. Positrons were longitudinally spin-polarized with polarization of 65 %. The sign of magnetic field is defined as positive (negative) when the field direction is the same as (opposite to) the polarization. Positron lifetime measurements were carried out using a conventional analog system and a ^{22}NaCl source in a magnetic field of ±1 T. The source was sandwiched by the above samples and a well annealed Cu. Subsequently, the source-sample was put into a gap of two permanent magnets. By subtracting the Cu bulk lifetime from the first lifetime component, the bulk lifetimes of the above samples were obtained as $\tau_{\pm}=2\tau_1-\tau_{Cu}$ (=115 ps). Subsequently, the spin dependent annihilation rates were obtained by Eqs. (2) and (3). All the above details are described elsewhere [2, 3, 9].

The differential DBAR spectra for individual bands were theoretically calculated. The electron wave functions were obtained from the ABINIT computation [10] with the projector-augmented-wave method [11]. The initial valence electron configurations were assumed to be $3s^23p^63d^64s^2$ (Fe), $3s^23p^63d^74s^2$ (Co), $3s^23p^63d^84s^2$ (Ni), $3s^23p^63d^54s^2$ (Mn), $2s^22p^63s^23s^1$ (Al), $3s^23p^2$ (Si) and $5s^25p^64f^75d^16s^2$ (Gd). The positron wave function was calculated based on the two-component density functional theory. The Boroński-Nieminen enhancement factor was adopted [12]. The DBAR spectrum was obtained by double-integrating the momentum density with a Gaussian convolution having the full width at half maximum of 1.4 keV. The details were described elsewhere [2, 3].

The total annihilation rate of spin-up (spin-down) positrons were obtained to be $\lambda^{\Uparrow(\Downarrow)}$= 9.35 (8.47) ns^{-1} (Fe), $\lambda^{\Uparrow(\Downarrow)}$= 8.91 (8.48) ns^{-1} (Co), $\lambda^{\Uparrow(\Downarrow)}$= 9.71 (9.62) ns^{-1} (Ni), $\lambda^{\Uparrow(\Downarrow)}$=6.49 (5.29) ns^{-1} (Gd), $\lambda^{\Uparrow(\Downarrow)}$= 6.80 (6.58) ns^{-1} (CMS), $\lambda^{\Uparrow(\Downarrow)}$=6.76 (6.62) ns^{-1} (CMA) and $\lambda^{\Uparrow(\Downarrow)}$= 5.88 (5.53) ns^{-1}. Thus, spin-up positrons annihilate faster than spin-down positrons. This may simply reflect the higher density of majority over minority spin electrons. The fractional differences between spin-up and spin-down annihilation rates, i.e., $(\lambda^{\Uparrow}-\lambda^{\Downarrow})/(\lambda^{\Uparrow}+\lambda^{\Downarrow})$, were in agreement with those obtained by the density functional theory described above. For Ni, the sign of $\lambda^{\Uparrow}-\lambda^{\Downarrow}$ was opposite to the previous observation [9]. Since for Ni the difference between τ_{+} and τ_{-} was only ~1 ps, the experimental determination of the sign might be somewhat problematic.

Fig. 1 shows the differential DBAR spectra between majority and minority spin electrons for the Fe, Co, Ni and Gd samples with theoretical curves. As for the theoretical curves of Fe, Co and Ni, the indices are given for the bands composed of 3*d* and 4*s* electrons. For Gd, the indices correspond to the individual orbits. For the Fe sample, a bump at around p=0 m_0c and a shoulder at around p=5~6 m_0c are seen. For the Co sample, the intensity at around p=0 m_0c is significantly lost as compared to the Fe sample. The overall intensity of the Ni sample is further reduced than those of the Fe and Co samples. The Gd sample exhibits only a peak centered at p=0 m_0c. Agreement between experiment and theory is qualitatively good suggesting that the calculation is accomplished in adequate precision. Hence, the theory may be used to interpret the experimental results. For Fe, the positive polarization of the 4 th to 6 th bands overcompensate the negative polarization of the 1 st to 3 rd bands. In the cases of Co and Ni, the negative polarization of the lower bands has more contribution than the positive polarization of the higher bands. Consequently, the intensity in low momentum region is sufficiently reduced. Wakoh and Yamashita explained such an effect as a consequence of the *s*-*d* hybridization [13]. In the case of

Gd, all the 5*sp* bands show nearly no polarization. Except for one, thirteen 4*f* bands are positively polarized since the minority spin bands have no states below the Fermi level. These 4*f* bands have only a small contribution probably because of less overlapping of positron and electron wave functions. One 4*f* minority spin band has states near the Fermi level and the corresponding differential spectrum is negatively polarized. Probably, positron wave function overlaps more with the wave function of this minority spin band because of the *f*-*d* hybridization. The Gd spectrum is composed mostly of 5*d* and 6s bands.

Fig. 2 (Left) shows the differential DBAR spectra between majority and minority spin electrons for the CMS, CMA and NMS samples. First, we compare the CMS and CMA samples. For the CMS sample, a bump at around p=0 m_0c and a shoulder at around p=10 m_0c are seen. For the CMA sample, the intensity at around p=0 m_0c is significantly lost. Contrarily to the CMS sample having $L2_1$ structure, the CMA sample is in fully disordered B2 structure. Therefore, one may consider that the reduced intensity of the CMA sample at around p=0 m_0c is due to the B2 disordering. Furthermore, the above difference between the CMS and CMA samples may be correlated with the general trend that CMS has a higher half-metallicity as compared to CMA [14]. However, the above argument is not true as explained below. The solid lines in Fig. 2 for CMS and CMA are theoretical curves assuming $L2_1$ structure. The blue (thin solid) and red (broken) lines represent positive and negative polarizations, respectively. Agreement between experiment and theory is good even if the CMA sample is in fully B2 structure. This indicates that the band structure and hence the electron momentum distribution is not dramatically changed between $L2_1$ and B2 structures [15]. Actually, our calculation supported this assumption. The bump at around p=0 m_0c and the shoulder at around p=10 m_0c for the CMS sample is interpreted as that, the total intensity of the positively polarized 17 th to 19 th bands having *sp*-like dispersion and the 13 th to 16 th bands having *d*-like dispersion overcompensate the total intensity of the other negatively polarized bands. In the case of the CMA sample, the 13 to 16 th bands are similarly positively polarized, but, the 17 th to 19 bands have nearly no states. Consequently, their total intensity does not exceed the total intensity of the other negatively polarized bands and hence the valley at around p=0 m_0c appears. As seen from the calculated band structures in Fig. 2 (Right), CMS has theoretically better half-metallicity as compared to CMA. Thus, considering the above arguments, it is concluded that, (i) from the agreement between experiment and theory, the CMS sample has a higher half-metallicity than the CMA sample and (ii) the half-metallicity is robust for the disordering from $L2_1$ to B2 structures.

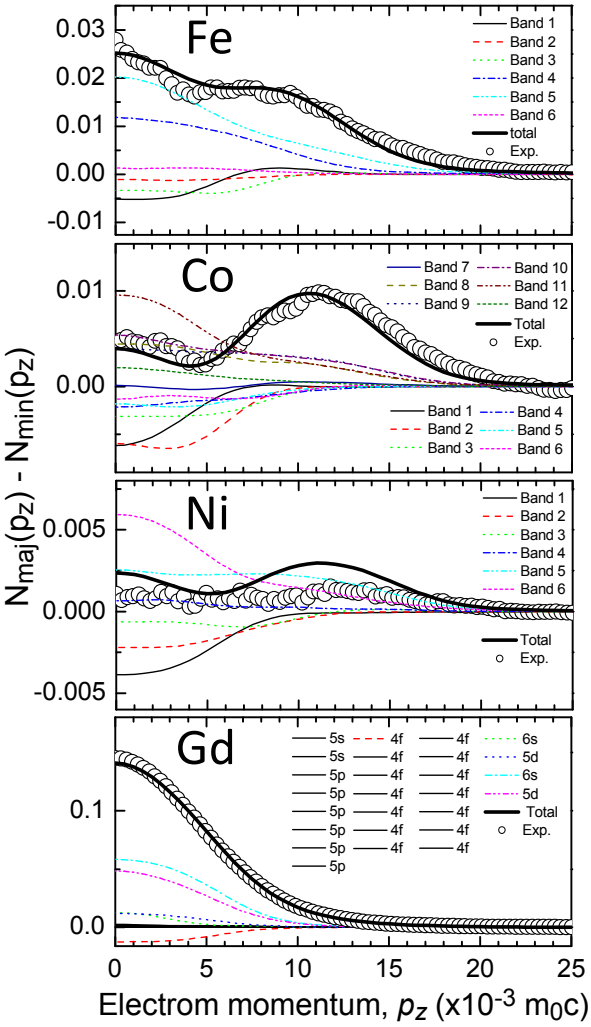

Fig. 1 Differential DBAR spectra between majority and minority spin bands for the Fe, Co, Ni and Gd samples and theoretical curves.

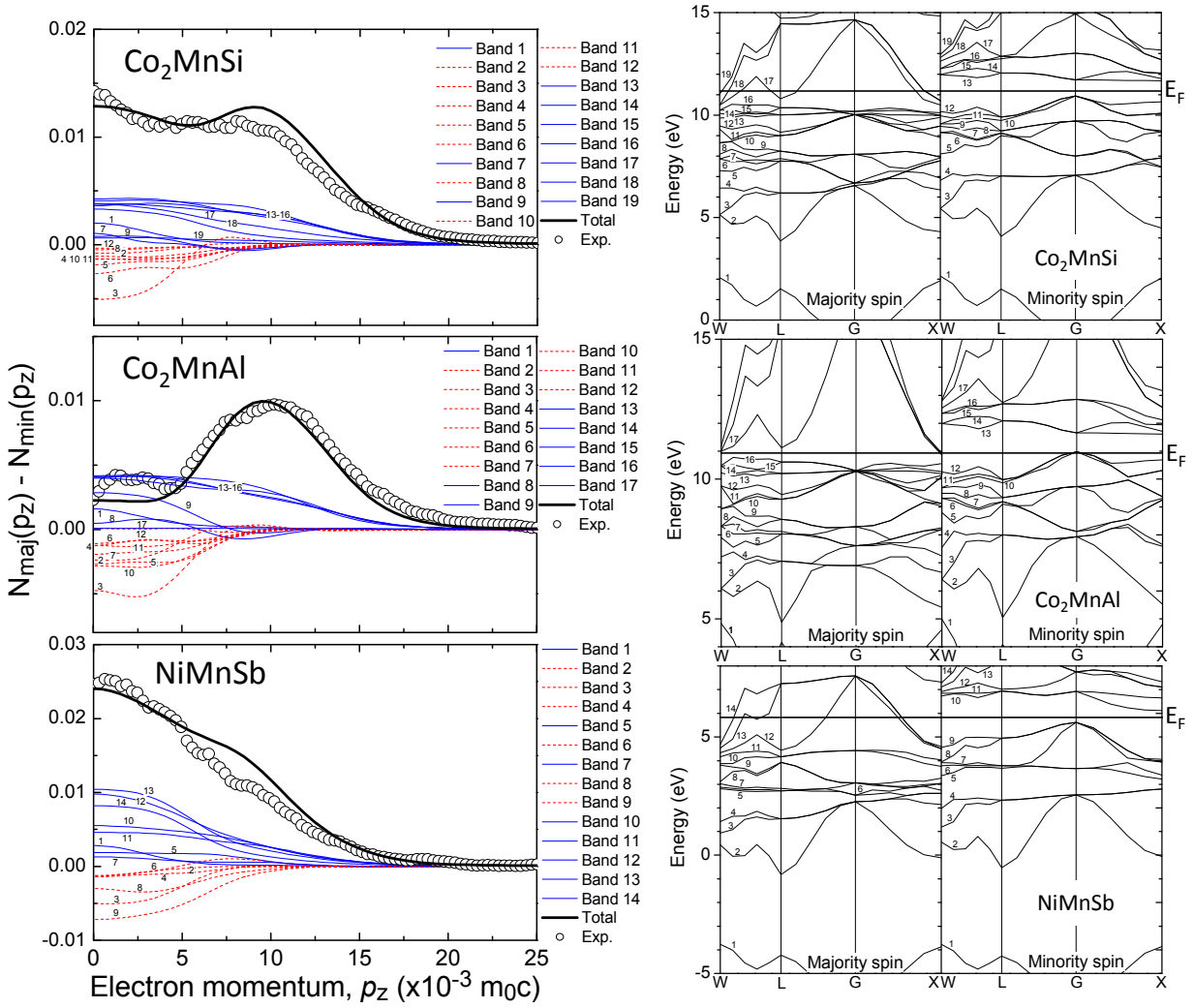

Fig. 2 Left: Differential DBAR spectra between majority and minority spin bands for the CMS, CMA and NMS samples and theoretical curves. Red (broken) and blue (thin solid) denote negative and positive polarization, respectively, for each band. Thick solid curves are the totals. Right: Theoretical band structures of CMS, CMA and NMS. E_F denotes the Fermi level.

Comparing the CMS sample, the NMS sample exhibits a more pronounced broad peak centered at p=0 m_0c. Again, the experimental is reproduced by the calculation. In the similar way as above, the experimental feature is explained in terms of the positively polarized 12 th to 14 th bands having *sp*-like dispersion that overcompensate the contributions from the other bands. Fig. 2 shows that NMS is theoretically good half-metal. The agreement between experiment and theory suggests that the NMS sample maintains half-metallicity which is as good as CMS [16].

Surface positronium annihilation

In this section, we describe the determination of surface spin polarization based on positronium annihilation. A portion of positrons implanted into a metal diffuse back to the surface and is emitted as positronium into vacuum. When both positrons and electrons are polarized, the intensities of spin-singlet and spin-triplet positronium exhibit asymmetry upon reversal of the spin polarization of positrons or electrons. Let us consider three-gamma events of spin-triplet positronium in the energy spectrum of annihilation radiation, since two-gamma events are hardly distinguished from free positron annihilation inside. The increment of the intensity in the lower energy part below the 511 keV peak from the background, denoted as ΔR, is proportional to the three-gamma annihilation intensity. Its asymmetry upon electron spin flip ($+P_- \Leftrightarrow -P_-$) is given by

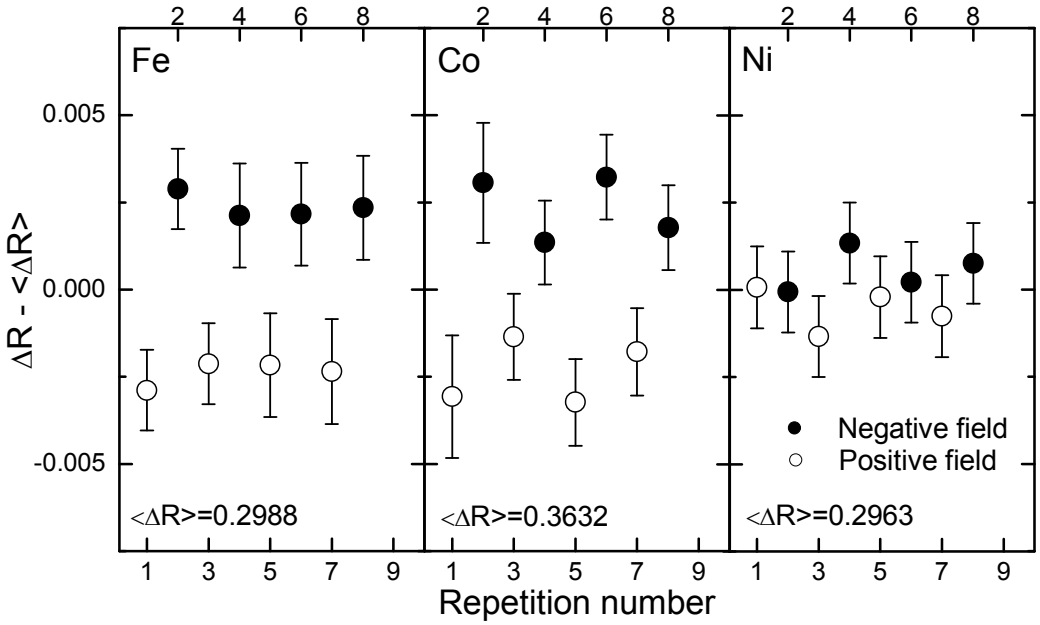

Fig. 3 Δ*R* values obtained for the Fe, Co and Ni samples as a function of successive application of opposite magnetic fields. Filled and open circles denote negative and positive magnetic fileds, respectively. <Δ*R*> denotes the average of Δ*R* values.

$$A^{3\gamma} = \frac{\Delta R(+P_-) - R(-P_-)}{\Delta R(+P_-) + R(-P_-)} = \frac{2\varepsilon(1) - \varepsilon(0)}{2\varepsilon(1) + \varepsilon(0)} P_+ P_- \cos\varphi, \tag{4}$$

where $\varepsilon(1)$ and $\varepsilon(0)$ are the detection efficiencies of annihilation gamma-rays from $m=\pm 1$ and $m=0$ (m denotes the magnetic quantum number of Ps), respectively, φ is the angle between positron and electron polarization directions [6].

Here, we prepared Fe(001), Co(001) and Ni(001) films of 500 nm thick on MgO(001) substrates by a physical vapor deposition in a vacuum chamber. From the reflection high-energy electron diffraction patterns and the x-ray diffraction 2θ curves, these samples are single crystals of bcc (Fe) and fcc (Co and Ni) structures. After transferring the samples to a UHV chamber (base pressure of less than $5\text{x}10^{-8}$ Pa) connected to a positron beam apparatus, the sample surfaces were cleaned by an Ar ion sputtering and heat treatment at 700°C. In the Auger electron spectroscopy analysis, oxygen and carbon peaks were sufficiently removed after the sputtering treatment. The samples were further put into the main chamber of the beam apparatus and in-plane magnetized by two Helmholtz coils placed outside the chamber. The magnetic field at the sample position was 20 mT. A transversely spin-polarized positron beam with energy of 50 eV and polarization of 47 % was generated using a ^{68}Ge-^{68}Ga source and conventional electrostatic beam system. Using a Ge detector, the value of Δ*R* was measured with repeatedly changing the field direction. The sign of magnetic field is positive (negative) when the field direction is the same as (opposite to) the positron polarization.

Fig. 3 shows Δ*R* values measured for the Fe, Co and Ni samples in positive and negative fields. For the Fe and Co samples, the difference between positive and negative fields is significant, while it is very small for the Ni sample. From Eq. 4 and the observed Δ*R*, the surface spin polarizations were obtained to be −2.6% (Fe), −2.1% (Co) and −0.5% (Ni). The sign and magnitude of the above surface polarizations are consistent with the early experiment [5]. The negative spin polarization means that more majority spin electrons are detected.

Considering a theoretical study about spin-polarized density of states (DOS) [17], at the first surface layer and at the Fermi level, minority spin electrons have more states than majority spin electrons. Therefore, the above results are hardly explained considering electrons only at the Fermi level. The positronium work functions for Fe, Co and Ni are −3.0 eV, −2.6 eV and −2.6 eV, respectively. If we simply integrate the theoretical DOS below the Fermi level with these energy widths, the spin polarizations for Fe, Co and Ni are roughly −30%, −10% and −5%, respectively. The

observed sign of spin polarization may be explained assuming that positrons pick up electrons located below the Fermi level. However, the order of magnitude of the observed spin polarization is still not explained. Positronium will be formed in the vacuum region at the surface, where the electron density is sufficiently reduced [18]. The theories suggest that, in such region, the spin polarization is further reduced [19, 20]. To fully explain the experiment, therefore, the positronium formation process should be revealed with detailed electronic and positronic states from the vacuum region to the bulk. Furthermore, new experimental techniques, such as spin-polarized positronium time-of-flight method that can provide spin-polarized DOS, need to be developed.

Acknowledgement

This work was finanncially supported by JSPS KAKENHI under Grant No. 24310072.

References

[1] S. Berko, Positron Annihilation in Ferromagnetic Solids, in: A. T. Stewart and L. O. Roellig (Eds.), Positron Annihilation, Academic Press, New York, 1967, pp. 61-79.

[2] A. Kawasuso, M. Maekawa, Y. Fukaya, A. Yabuuchi, and I. Mochizuki, Phys. Rev. B83 (2011)100406(R).

[3] A. Kawasuso, M. Maekawa, Y. Fukaya, A. Yabuuchi and I. Mochizuki, Phys. Rev. B85 (2012)024417.

[4] S. Berko and A. P. Mills, J. Phys. Colloques 32(1971) C1-287.

[5] D. W. Gidley and A. R. Koymen, Phys. Rev. Lett. 49(1982)1779.

[6] A. Kawasuso, Y. Fukaya, M. Maekawa, H. Zhang, T. Seki, T.Yoshino, E. Saitoh, K. Takanashi, J. Mag. Mag. Mater. 342(2013)139.

[7] H. J. Zhang, S. Yamamoto, Y. Fukaya, M. Maekawa, H. Li, A. Kawasuso, T. Seki, E. Saitoh& K. Takanashi, Scientific Reports 4, (2014) 04844.

[8] H. J. Zhang, S. Yamamoto, B. Gu, H. Li, M. Maekawa, Y. Fukaya, and A. Kawasuso Phys. Rev. Lett. 114(2015)166602.

[9] H. Li, M. Maekawa, A. Kawasuso and N. TanimuraJ. Phys. Condens. Matter 27(2015)246001.

[10] X. Gonze *et al.*, Comput. Mater. Sci. 25(2002)478.

[11] P. E. Blöchl, Phys. Rev. B 50(1994)17953.

[12] E. Boroński and R. M. Nieminen, Phys. Rev. B 34(1986)3820.

[13] S. Wakoh and J. Yamashita, J. Phys. Soc. Jpn. 21(1966)1712.

[14] S. Ishida, S. Fujii, S. Kashiwagi and S.Asano, J. Phys. Soc. Jpn. 64(1995)2152.

[15] Y. Miura, K. Nagao and M. Shirai, Phys. Rev. B69(2004)144413.

[16] K. E. H. M. Hanssen, P. E. Mijnarends, L. P. L. M. Rabou, K. H. J. Buschow, Phys. Rev. B42(1990)1533.

[17] C. H. Park, B. C. Lee and J. I. Lee, J. Kor. Phys. Soc. 47(2005)655.

[18] A. Held and S. Kahana, Can. J. Phys. 42(1964)1908.

[19] E. Wimmer, A. J. Freeman and H. Krakauer, Phys. Rev. B30(1984)3113.

[20] R. Wu and A. J. Freeman, Phys. Rev. Lett. 69(1992)2867.